Journal of Inflammation Research

Dovepress
Taylor & Francis Group

Open Access Full Text Article

ORIGINAL RESEARCH

Spermidine Exerts Neuroprotective Effects Following Intracerebral Hemorrhage in Mice Through Anti-Inflammation and Blood-Brain Barrier Protection

Lingxiao Qi[1,2], Xiangyu Zhang[1,2], Yuanyuan Liu[1,2], Pingping Guo[1,2], Rabeea Siddique[1,2], Maham Mazhar[1,2], Sara Xue[3], V Wee Yong[3], Mengzhou Xue[1,2]

[1]Department of Cerebrovascular Diseases, The Second Affiliated Hospital of Zhengzhou University, Zhengzhou, Henan, People's Republic of China; [2]Academy of Medical Science, Zhengzhou University, Zhengzhou, Henan, People's Republic of China; [3]Hotchkiss Brain Institute and Department of Clinical Neurosciences, University of Calgary, Calgary, Alberta, Canada

Correspondence: V Wee Yong, Hotchkiss Brain Institute and Department of Clinical Neurosciences, University of Calgary, Calgary, Alberta, Canada, Email vyong@ucalgary.ca; Mengzhou Xue, Department of Cerebrovascular Diseases, The Second Affiliated Hospital of Zhengzhou University, 2 Jingba Road, Zhengzhou, Henan, 450001, People's Republic of China, Email xuemengzhou@zzu.edu.cn

Purpose: Intracerebral hemorrhage (ICH) is a life-threatening subtype of stroke, and neuroinflammation is a key factor in brain injury after ICH. Spermidine (SPD), a natural polyamine existing in all eukaryotic cells, has exerted beneficial effects such as anti-inflammation and anti-oxidation in many disease models. However, its effects and mechanisms in ICH remain unclear. This study aims to investigate the therapeutic potential of SPD in the ICH model.

Methods and Materials: In the in vivo experiments, C57BL/6 mice were randomly divided into three groups (Sham group, ICH + vehicle group, and ICH + SPD group). ICH was induced by collagenase VII and SPD (15 mg/kg) was administered intraperitoneally at 6, 30, and 54 hours post-ICH. Then the mice were euthanized on the third day for further experiments: Western blot, immunofluorescence staining, immunohistochemical staining, Evans blue extravasation, TUNEL staining, brain water content measurement and behavioral tests. In in vitro experiments, BV2 cells were stimulated with hemin for 24 hours to mimic ICH. Western blot and ELISA were used to assess inflammatory response of microglia.

Results: The results of animal experiments showed that SPD dramatically reduced hematoma volume, area of brain injury, brain cell death, and significantly improved neurological deficits compared with the ICH + vehicle group. Furthermore, SPD suppressed the activated microglia/macrophages, infiltrated neutrophils and the expression of inflammatory cytokines (IL-1β, IL-6, and TNF-α), alleviated blood-brain barrier (BBB) damage, and reduced brain water content in vivo. In cell experiments, the results indicated that SPD (8 μM/L) suppressed the expression of CD32 and iNOS and the release of inflammatory factors (IL-1β, IL-6, and TNF-α).

Conclusion: These findings indicate the neuroprotective role of SPD in the ICH model in mice, which is likely to be associated with inhibition of neuroinflammation and protection of the BBB.

Keywords: intracerebral hemorrhage, spermidine, neuroinflammation, blood-brain barrier

Introduction

Intracerebral hemorrhage (ICH) is a fatal cerebrovascular disease, accounting for 10–15% of all strokes. Each year, approximately 2 million people worldwide suffer from ICH.[1,2] Roughly 40% of them die within the first month, and the survivors often have neurological dysfunctions of varying degrees.[1,2] Additionally, ICH often occurs in elderly populations with hypertension.[3] With the development of aging, many elderly individuals suffer from hypertension and use anticoagulants for a long time, leading to an increase in the number of hospitalizations for ICH.[4,5]

The adverse prognosis of ICH is the consequence of the joint action of primary and secondary brain injuries.[6] The mechanical effect caused by the hematoma after ICH leads to primary brain injury. Subsequently, blood components

Received: 27 January 2025
Accepted: 17 May 2025
Published: 7 June 2025

including erythrocyte fragments and degradation products accumulate in the brain tissues, immediately activating resident microglia. Together with the infiltrating leucocytes, they release pro-inflammatory cytokines and toxic molecules.[7,8] This disrupts the integrity and increases the permeability of blood-brain barrier (BBB), aggravating the development of perihematomal edema (PHE).[9,10] Research indicates that PHE enhances the mass effect caused by the initial hematoma, causing direct damage to brain tissue.[11] Meanwhile, BBB disruption also promotes inflammation by facilitating infiltration of leucocytes, further exacerbating brain edema and brain tissue injury after ICH.[12] The secondary brain injuries following ICH last for several days or even weeks.[13] Minimally invasive surgery is currently used to alleviate mechanical damage caused by hematoma accumulation in the early stages of ICH, but there is still a lack of effective drugs to ameliorate secondary brain injury.[7,14]

Spermidine (SPD) is a natural polyamine existing in all eukaryotic cells, which regulates various cellular processes such as growth, proliferation, differentiation, and aging.[15–17] Clinical trials have indicated that oral SPD supplements are safe and well tolerated.[18] In mouse models of neurological diseases, SPD exerts broad neuroprotective effects by exhibiting anti-inflammatory and anti-oxidative properties.[19–21] In the BV2 microglial cell model stimulated by lipopolysaccharide (LPS), SPD pretreatment suppressed the activation of microglia and the production of pro-inflammatory and neurotoxic molecules.[22] However, it remains uncertain that how SPD regulates inflammatory response and whether it exerts neuroprotective effects following ICH. This study explored the therapeutic effects of SPD in a mouse model of ICH, with the aim of providing a potential treatment strategy for mitigating the secondary brain injury after ICH.

Materials and Methods

Animal Experiments

Animals

C57BL/6 mice, aged 8–10 weeks, weighing 20–25 grams, were purchased from Beijing Vital River Experimental Animal Centre. These mice were housed in an SPF-level animal experimental center and maintained in suitable conditions of room temperature 25 °C, relative humidity 55%, and a 12-hour light-dark cycle, with sufficient oxygen, food and water. All animal experiment procedures in this study were approved by the Ethics Committee of the Second Affiliated Hospital of Zhengzhou University.

ICH Models and SPD Administration

As previously mentioned, the ICH surgical model was created by injecting collagenase VII (Sigma, St Louis, MO, USA) into the right striatum of mice.[23] First, we anesthetized mice with isoflurane-oxygen mixture, and then incised their scalp. Subsequently, the mice were fixed onto a brain stereotaxic apparatus (RWD, Shenzhen, China), and a small hole was drilled in the skull at the designated coordinates (0.8 mm in front of the bregma, 2.0 mm lateral to the midline). Next, 0.075 U collagenase VII dissolved in 0.75 μL saline was vertically and slowly injected into the drilling position at a rate of 0.1 μL/min. The needle was kept in place for 10 minutes before removal to prevent backflow. Finally, the drill hole was sealed with bone wax, and the scalp incision was sutured. Mice in the sham group were injected with an equal volume of saline. Sterile practices were meticulously maintained throughout the surgery.

The mice were randomly divided into 3 groups: Sham group, ICH + vehicle group and ICH + SPD group. SPD (S0266) was purchased from Sigma-Aldrich (St. Louis, Missouri, USA). SPD was dissolved in saline and administrated intraperitoneally to the mice with a dose of 15 mg/kg at 6 hours, 30 hours, and 54 hours after the induction of ICH.[24,25] The mice in the vehicle group were injected with the corresponding volume of saline based on their body weight at the same time. The dosing intervals was designed to intervene early in inflammatory cascades (6 hours) and maintain therapeutic efficacy through the peak of neuroinflammation (72 hours), as demonstrated in prior ICH study.[26] This regimen is also supported by studies of SPD treatment in murine traumatic brain injury (TBI) models.[25]

Brain Tissue Preparation

Typically, activated microglia/macrophages and infiltrated neutrophil peak at 3 days after ICH,[26] and the most severe BBB disruption also occurs on the third day after ICH.[27] Therefore, brain specimens were collected 72 hours after ICH induction. After anesthetizing mice, the perihematomal brain tissues were harvested for subsequent Western blot

experiments. After perfusing the heart with saline solution and 4% paraformaldehyde, the mouse brains were immediately removed and fixed in tissue fixative solution for 3–5 days. For staining experiment, fixed brains were serially sliced into 5 μm paraffin sections through the needle entry site.

Hematoma Volume Measurement

The hematoma volume on the third day after ICH was measured according to the method previously reported by our group, with slight modifications.[28] The brain was cut into 1 mm-thick coronal slices and photographed. The following formula is used to calculate the total volume of the hematoma: Hematoma volume (mm^3) = the sum of the areas of each section (mm^2) × thickness (mm).[29]

Behavioral Tests

Modified Neurological Severity Scores (mNSS)

As previously reported, the mNSS was used to assess functional impairment.[30] In this experiment, two researchers who were blinded to the experimental conditions, scored the mice on their motor, sensory, balance, and reflex tests according to the scoring criteria 24 hours and 72 hours after ICH induction. The scoring range was 0–18, with higher scores indicating more severe neurological deficits.

Corner Turn Test

The mouse's preference for turning after entering a corner can reflect the sensory and motor impairments caused by unilateral striatum damage. During the experiment, two thick glass plates were placed vertically on the table surface and formed an angle of 30 degrees, with the open end located at the edge of the table When mice tested entered the deep part of the corner, both sides of their whiskers were stimulated, so they turn left or right. Recording the number of times when they turn right. Corner test score = [(R / (R + L)] × 100%.[31]

Western Blot Analysis

Briefly, RIPA lysis buffer (Solarbio, China) was added based on brain tissue's weight, followed by homogenization and centrifugation. Then, the protein concentration of the supernatant was determined using the BCA protein assay kit (Beyotime, China). Equal amounts of proteins were electrophoresed and transferred onto a polyvinylidene fluoride (PVDF) membrane (Merck KGaA, Darmstadt, Germany). Subsequently, the membrane was blocked to prevent non-specific binding and then incubated with the primary antibody overnight at 4°C. Primary antibodies against Iba-1 (1:1000), myeloperoxidase (MPO) (1:1000), tumor necrosis factor-α (TNF-α) (1:1000), interleukin-6 (IL-6) (1:1000), CD32 (1:1000), matrix metalloproteinases-9 (MMP-9) (1:1000) and occludin (1:1000) were purchased from Abcam (Cambridge, MA, UK). Primary antibodies against inducible nitric oxide synthase (iNOS) (1:1000), nuclear factor-κB (NF-κB)-P65 (1:1000) and phospho-NF-κB-P65 (1:1000) were purchased from Cell Signaling Technology (USA). Primary antibody against interleukin-1β (IL-1β) (1:1000) was purchased from R&D systems (USA). Primary antibody against GAPDH (1:5000) was purchased from HUABIO (Hangzhou, China). Primary antibody against zonula occludens-1 (ZO-1) (1:5000) and Albumin (1:1000) was purchased from Proteintech (Wuhan, China). On the second day, the membrane was incubated with the corresponding horseradish peroxidase (HRP)-conjugated secondary antibody (anti-rabbit or anti-mouse) at room temperature for 1 hour. The secondary antibody was purchased from Servicebio (Wuhan, China). Finally, the protein bands were visualized by adding the enhanced chemiluminescence (ECL, Beyotime Institute of Biotechnology) and using the BIO-RAD ChemiDoc™ MP imaging system (original full-length Western blot images are provided in supplementary materials).[32]

Immunofluorescence Staining

Paraffin sections were routinely deparaffinized with xylene and rehydrated with ethanol. Antigen retrieval was then performed by incubating the sections in a 10 mm sodium citrate solution at 100°C for 3 minutes and 40°C for another 15 minutes. After cooling, the sections were blocked in 5% bovine serum albumin for 30 minutes at room temperature. The brain sections were incubated with the primary antibody at 4°C overnight. The primary antibodies included rabbit anti-Iba1 (1:200, Abcam, Cambridge, MA, USA), rabbit anti-ZO-1 (1:100, Abcam, Cambridge, MA, USA), Goat anti-platelet endothelial cell adhesion

molecule-1 (CD31) (1:100, R&D systems, USA) and mouse anti-Neuron (NeuN) (1:1000, Abcam, Cambridge, MA, USA). On the second day, after rinsing with PBS (pH = 7.4) thrice, the samples were incubated at room temperature in the dark for 1 hour with the secondary antibody (1:200, Alexa Fluor 594 and Alexa Fluor 488) purchased from Abbkine (California, USA). After all the sections were mounted, images were captured using a fluorescence microscope (Olympus Co., Tokyo, Japan) under uniform shooting conditions and the number of positive cells was counted by Image J.[33]

Immunohistochemical Staining

After dewaxing and rehydration, brain sections were sequentially incubated with 3% hydrogen peroxide for 15 minutes to remove endogenous peroxidase. Then, citrate buffer was used for antigen retrieval and 5% goat serum was used for blocking. The sections were incubated with primary antibodies against MPO (1:800, Abcam, Cambridge, MA, USA) at 4°C overnight. The following day, they were incubated with HRP-combined secondary anti-rabbit immunoglobulin G (IgG) antibody (1:800, Servicebio, Wuhan, China) for 1 hour at room temperature. The sections were stained with diaminobenzidine and hematoxylin. After dehydration, sections were sealed, and observed under a microscope.

Brain Water Content Measurement

The brain water content was assessed by the wet/dry method. On the third day after ICH, mice were euthanized and the brains were directly removed after decapitation. The olfactory bulbs and lower brain stems were removed, and the remaining cerebellum, contralateral hemisphere and ipsilateral hemisphere were weighed separately, which was defined as the wet weight. Subsequently, they were placed in an oven at 100°C for 24 hours to obtain the dry weight. The formula for calculating brain water content (%) was: (wet weight - dry weight) / wet weight × 100%.

BBB Permeability Assay

The relative amount of Evans Blue (EB) dye in brain tissue reflects changes in the permeability of the BBB.[28,34] On the third day following ICH, mice were fixed on a tail vein injection device and injected with 2% EB dye (4 mL/kg). Three hours later, heart perfusion with 0.9% saline was performed on the mice. Subsequently, the brain tissues were extracted and divided into left and right hemispheres. Each hemisphere was homogenized in formamide at a ratio of 1:10 and placed in a 60°C water bath for 24 hours, and then centrifuged at 1000 rpm for 10 minutes to collect the supernatants. Finally, measured the absorbance of the supernatants at a wavelength of 610 nm and calculated the EB concentration. The experimental results were presented as the ratio of the EB content in the ipsilateral to the contralateral brain.

Hematoxylin and Eosin (HE) Staining

HE staining was used to demonstrate the edema and necrosis of cells in the tissues surrounding the hematoma after ICH. Paraffin sections were processed following the protocol recommended in the instructions, and the modified HE staining kit used was purchased from Solarbio (Beijing, China).

Terminal Deoxynucleotidyl Transferase-dUTP Nick-End Labeling (TUNEL) Staining

To quantitatively analyze the degree of brain cell death (including necrosis and cell apoptosis), TUNEL was conducted according to the manufacturer's instructions of the TUNEL FITC Apoptosis Detection Kit (Vazyme, Nanjing, China). To further determine neuronal death, we performed immunofluorescence co-staining of NeuN (the neuronal marker) and TUNEL. Once the slides were sealed, the sections were observed and imaged using a fluorescence microscope (Olympus Co., Tokyo, Japan). Positive cells were counted with Image J.

Cell Experiments

Culture and Treatment of BV2 Cells

BV2 cells are immortalized mouse microglia line. Both the cells and the dedicated culture medium were purchased from Procell (Wuhan, China). The cells were incubated in a humidified incubator at 37°C with 5% CO_2 and the culture medium was refreshed every 2 days. Hemin (HY-19424, MedChemExpress) was dissolved in 0.1M NaOH and SPD was dissolved in saline. Hemoglobin is a major component of blood and is released from lysed erythrocytes after ICH and the hemin-treated cell model is a classical model for simulating brain cell damage after ICH.[35] So, the in vitro ICH model was established by exposing BV2 cells to hemin solution.

Cell Grouping and Pharmacological Intervention

In this experiment, three groups were used: sham group, hemin group and SPD group. Control group: BV2 cells were normally cultured and no additional treatment required. Hemin group: The corresponding concentration of hemin was added to the culture medium of BV2 cells, and the treatment time was 24 hours. SPD group: Before the addition of hemin, the cells were pretreated with the prescribed concentration of SPD for 1 hour.

Cell Viability Assay

CCK-8 kit was purchased from Glpbio (GK10001, USA). As described previously, BV2 cells were seeded in 96-well plates at a density of 5000 cells per well. After the cells adhered, they were exposed to various concentrations of hemin (0, 40, 80, 100, 150, 200, 300, 400 μM/L) or SPD (0, 2, 4, 6, 8, 10, 20, 30 μM/L).[36,37] After 24 hours, 10 μL of CCK-8 solution was added to each well and incubated at 37°C for 2 hours. The absorbance was measured at 450 nm. Cell viability (%) = [(Experimental Wells - Blank Wells) / (Control Wells - Blank Wells)] × 100%.

Western Blot Analysis

After cell collection, lysis buffer was added at an appropriate ratio. The mixture was left on ice for 30 minutes before undergo sonication for complete lysis. Subsequently, the samples were centrifuged to obtain the supernatant. The detailed procedures for measuring protein concentration and performing Western blot can refer to the "Animal Experiments" section.

Enzyme-Linked Immunosorbent Assay (ELISA)

After 24 hours treatment with hemin, the cell culture medium was collected and centrifuged. Subsequently, the supernatant was collected and processed according to the manufacturer's instructions of detection kits for TNF-α (Clone Cloud, Wuhan, China), IL-6 (Multi Science, Hangzhou, China) and IL-1β (Invitrogen, Carlsbad, CA, USA). Finally, the absorbance value of each sample at 450 nm was measured using a microplate reader to calculate the concentration of the substances to be tested in the samples. There were 3 samples in each group, and each sample was tested 3 times.

Statistical Analysis

All results were shown as mean ± SD and the statistical analysis was performed by using GraphPad Prism 8.0.1. Differences among multiple groups are analyzed with one-way ANOVA or two-way ANOVA followed by Tukey's multiple comparisons test. $p < 0.05$ was defined as statistically significant.

Results

SPD Shrinks the Volume of Hematoma and the Area of Brain Injury

To assess the direct effect of SPD on brain injury, we calculated hematoma volume at 72 hours post-ICH. The results indicate that, compared with the ICH + vehicle group, the SPD treatment led to a significant reduction in the hematoma volume (Figure 1A and B). The HE staining showed that there was only a small amount of blood and slight edema around the striatum in the sham group mice. In the ICH+ vehicle group, a large number of red blood cells were present and the brain tissue around the hematoma was loose. However, after SPD treatment, these symptoms were significantly improved (Figure 1C and D). The quantitative results further indicated that SPD could effectively reduce the area of brain injury after ICH.

SPD Decreases the Number of Activated Microglia/Macrophages and the Infiltration of Neutrophils

We performed immunofluorescence staining of Iba-1 (a representative molecule of microglia) and immunohistochemical staining of MPO (a representative molecule of neutrophils) on paraffin sections. The results indicated that on the 72 hours after ICH, compared with the sham group, the number of activated microglia/macrophages and infiltrating neutrophils in the ICH + vehicle group significantly increased; compared with the ICH + vehicle group, treatment with SPD led to a decrease in the number of these two types of immune cells (Figure 2A–C). The Western blot experimental results showed the same trend (Figure 2D–F) (Figure S1). This suggests that SPD inhibits microglia/macrophage activation and neutrophil infiltration after ICH.

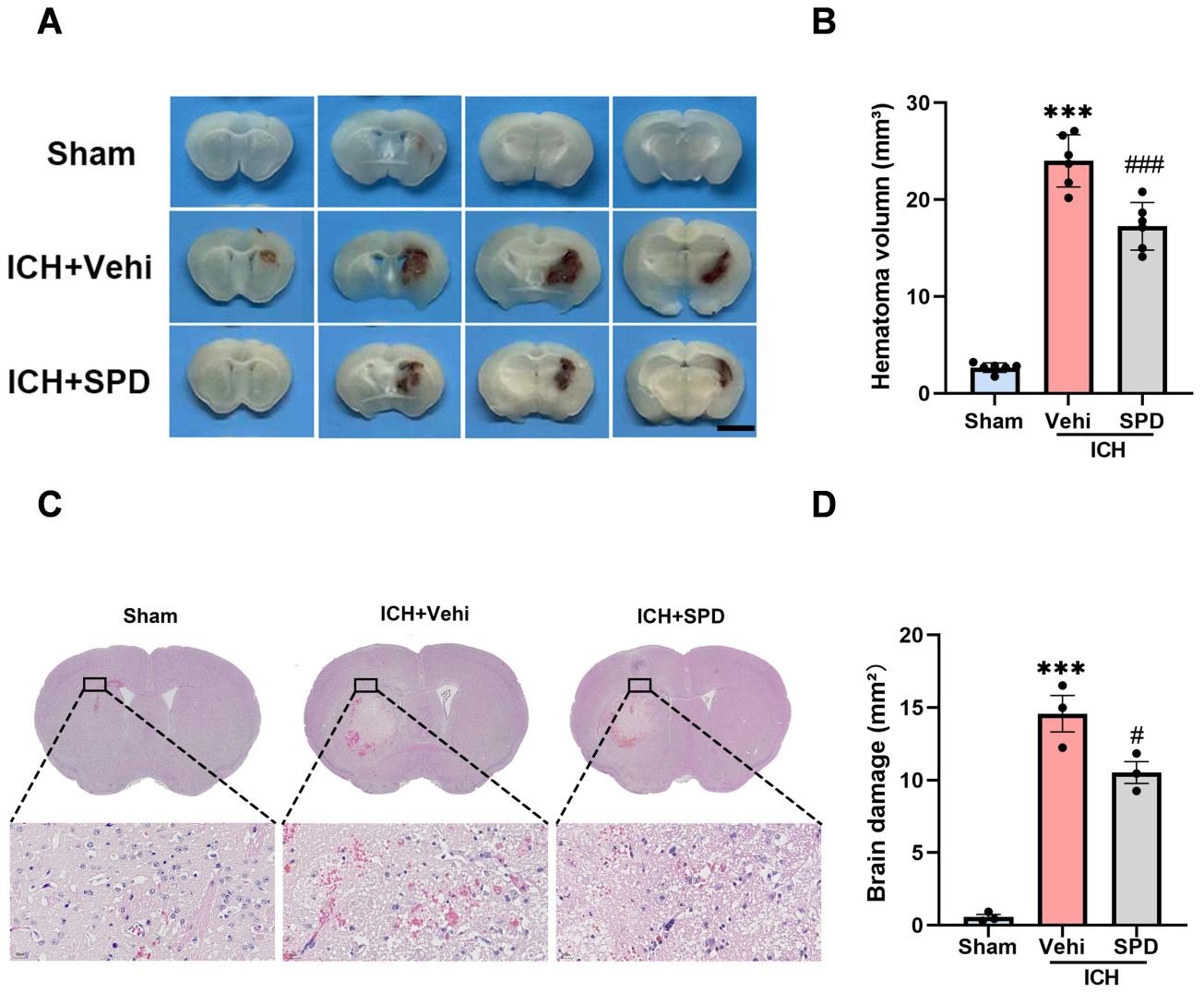

Figure 1 SPD reduces the volume of hematoma and the area of brain injury at 72 hours after ICH in mice. (**A**) Representative images of brain slices at 72 hours after ICH. Scale bar =2.5 mm. (**B**) The quantification results of hematoma volume, n = 6 per group. (**C**) Representative images of HE staining. Scale bar = 20 μm. (**D**) Quantification of the area of brain injury, n = 3 per group. ***p < 0.001 vs sham. #p < 0.05, ###p < 0.001 vs ICH + vehicle. Numerical data are shown as the mean ± SD. The difference between groups was analyzed using One-way ANOVA test.

SPD Reduces the Production Pro-Inflammatory Cytokines Following ICH

NF-κB is a nuclear transcription factor that plays a crucial role in neuroinflammation following ICH, and is capable of regulating inflammatory responses and the expression of inflammatory factors.[38] The Western blot results indicated that the expression of p-NF-κB was significantly elevated in the perihematomal region after ICH, while SPD suppressed its expression (Figure 3A and B) (Figure S2). TNF-α, IL-1β and IL-6 are inflammatory cytokines present in the brain tissue surrounding the hematoma. The Western blot results demonstrated that compared with the sham group, the production of the three cytokines in the tissue adjacent to the hematoma was markedly increased, while SPD treatment decreased their production (Figure 3C–H) (Figure S2).

SPD Inhibits the Inflammatory Response of Microglia Stimulated by Hemin

To further investigate the mechanism by which SPD inhibits the activation of microglia, we established an in vitro ICH model. Firstly, the CCK-8 results revealed that the viability of BV2 cells decreased by approximately 50%[35] when the hemin concentration was 150 μM/L. Hence, 150 μM/L was selected as the test concentration (Figure 4A). To determine the potential harmful effect of SPD on BV2 cells, SPD concentration gradient ranging from 0 to

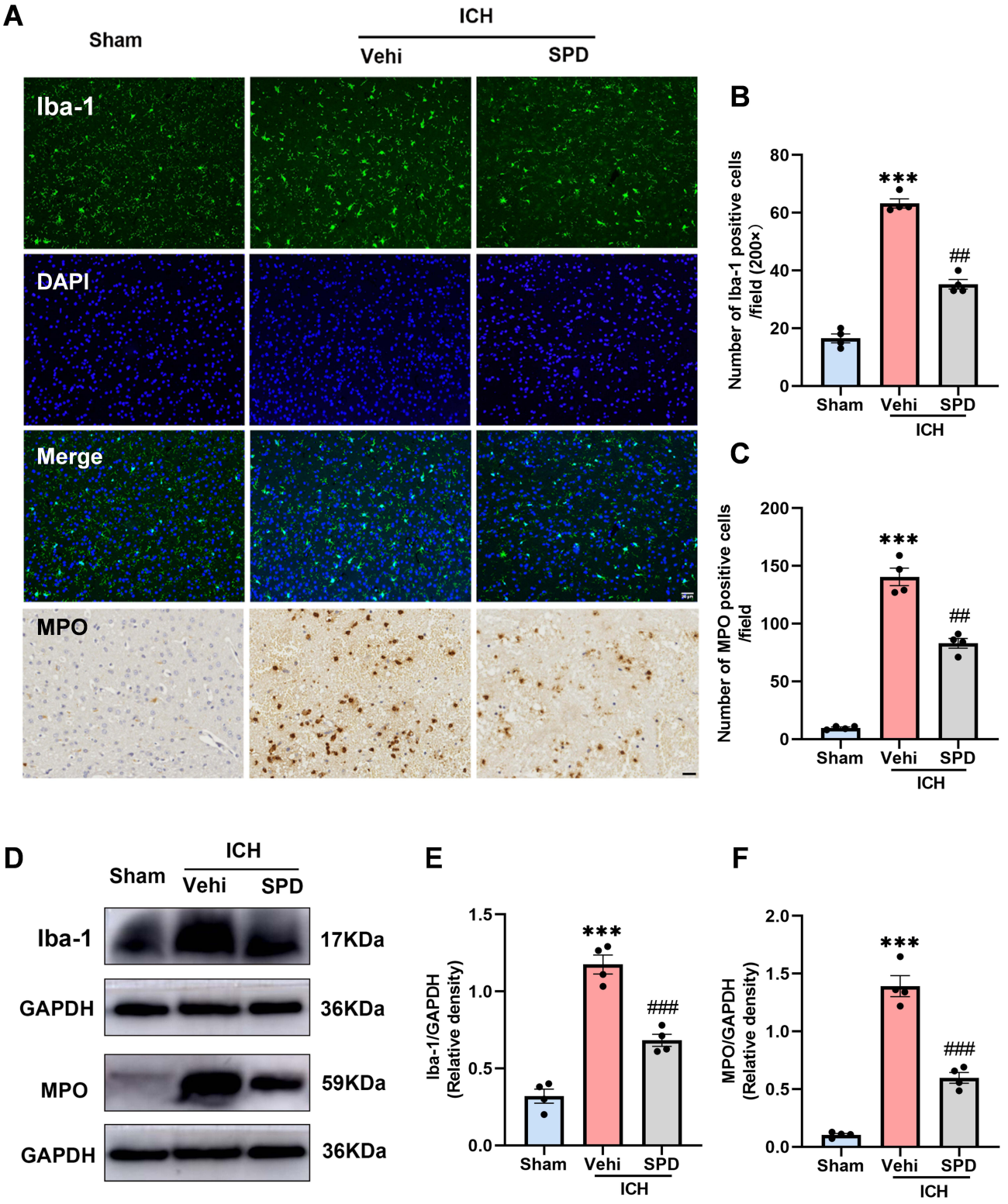

Figure 2 SPD alleviates the activated microglia/macrophages and infiltrated neutrophils at 72 hours after ICH in mice. (**A**) Representative immunofluorescence images of Iba-1 (Scale bar = 20 μm) and immunohistochemical images of MPO (Scale bar = 20 μm) in the peri-hematoma area at 72 hours after ICH. (**B** and **C**) Quantitative analysis of the number Iba-1 and MPO positive cells in each visual field. n = 4 per group. (**D**) Representative Western blot bands of Iba-1 and MPO. (**E** and **F**) Quantitative analyses of relative protein expression level of Iba-1 and MPO. n = 4 per group. ***p < 0.001 vs sham. ##p < 0.01, ###p < 0.001 vs ICH + vehicle. Numerical data are shown as the mean ± SD. The difference between groups was analyzed using One-way ANOVA test.

https://doi.org/10.2147/JIR.S515256

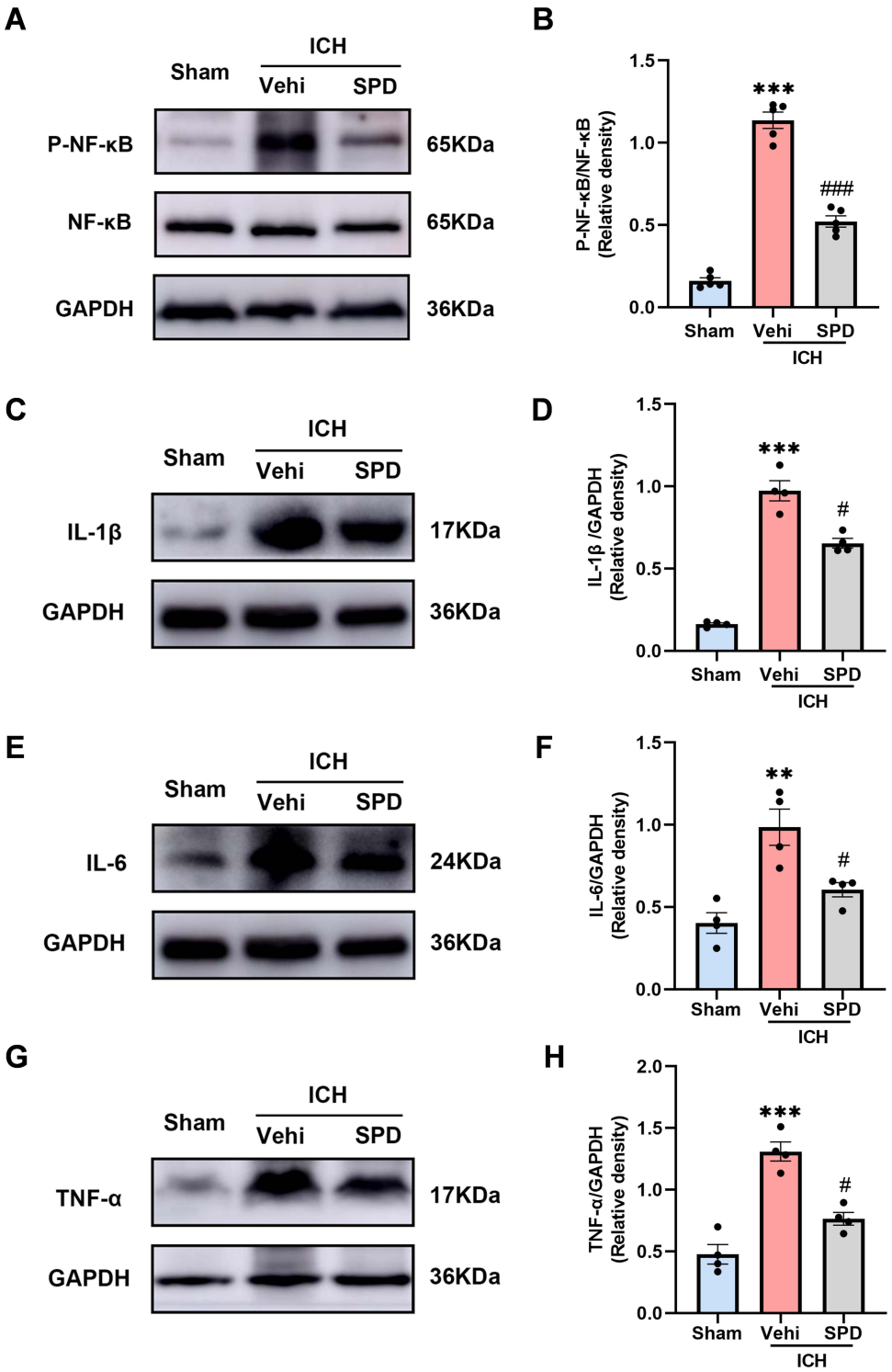

Figure 3 SPD attenuates the release of inflammatory cytokines in 72 hours models of mice with ICH. (**A**) Representative Western blot bands of P-NF-κB and NF-κB. (**B**) Quantitative results of P-NF-κB/NF-κB. n = 5 per group. (**C, E** and **G**) Representative Western blot bands of IL-1β, IL-6 and TNF-α. (**D, F** and **H**) Quantitative analyses of the levels of IL-1β, IL-6 and TNF-α at 72 hours after ICH. n = 4 per group. **p < 0.01, ***p < 0.001 vs sham. #p < 0.05, ###p < 0.001 vs ICH + vehicle. Numerical data are shown as the mean ± SD. The difference between groups was analyzed using One-way ANOVA test.

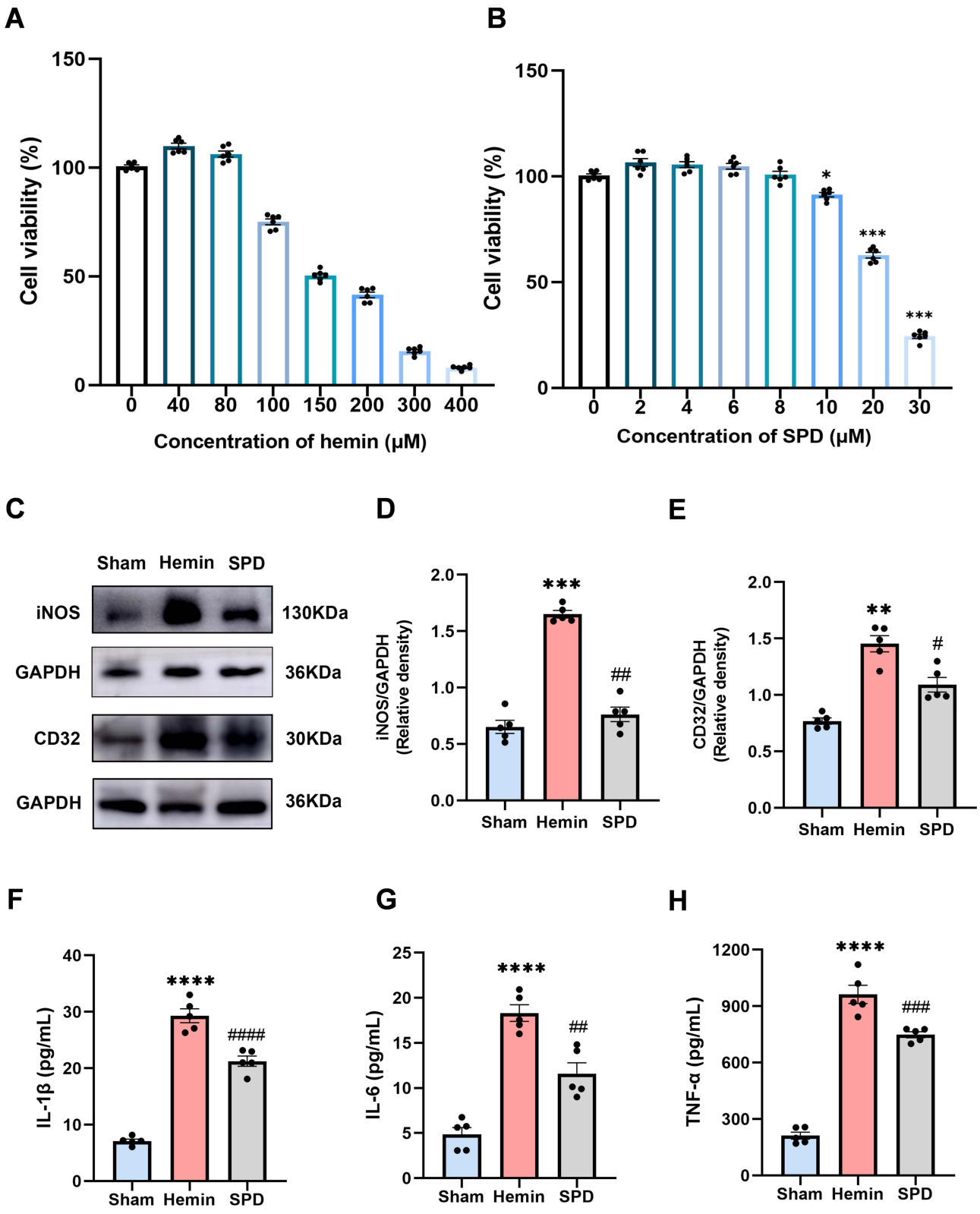

Figure 4 SPD inhibits the microglial cell inflammatory response stimulated by hemin in vitro. BV2 cell viability was measured by CCK8 after treated with (**A**) hemin (0–400 μM) or (**B**) SPD (0–30 μM) for 24 hours. n = 6 per group. (**C**) Representative Western blot bands of iNOS and CD32. (**D** and **E**) Quantitative analyses of relative protein expression level of iNOS and CD32. n = 5 per group. (**F**–**H**) Quantitative analysis of the levels of IL-1β, TNF-α, and IL-6 by the ELISA assay. n = 5 per group. *p < 0.05, ***p < 0.001 vs 0 μM. **p < 0.01, ***p < 0.001, ****p < 0.0001 vs sham. #p < 0.05, ##p < 0.01, ###p < 0.001, #####p < 0.0001 vs Hemin. Numerical data are shown as the mean ± SD. The difference between groups was analyzed using One-way ANOVA test.

https://doi.org/10.2147/JIR.S515256

30 μM/L was set for the CCK-8 assay. The results showed that 0, 2, 4, 6 and 8 μM/L SPD had no obvious effect on cell viability ($p > 0.05$), and SPD supplementation above 10 μM/L significantly decreased cell viability ($p < 0.05$) (Figure 4B). So, we chose 8 μM/L as an appropriate dose of SPD for the subsequent experiments. The Western blot results showed that the increased expression of iNOS and CD32 (the markers of pro-inflammatory microglia) induced by hemin was reversed by SPD treatment (Figure 4C–E) (Figure S3). Subsequently, the levels of inflammatory factors were detected by ELISA. The data indicated that hemin led to an increase in the levels of IL-1β, IL-6, and TNF-α secreted by BV2 cells. Compared with the hemin group, SPD decreased the secretion of inflammatory factors (Figure 4F–H). These results indicated that pretreatment with 8μM/L SPD appears to be effective in resisting hemin-induced inflammatory response of microglia.

SPD Reduces MMP-9 Levels and Protects the Integrity of the BBB

The brain capillary endothelial cells and tight junction proteins (TJPs) serve as crucial indicators for maintaining the integrity of the BBB.[39] MMP-9 participates in the disruption of the BBB after ICH.[40] Western blot results revealed that, in contrast to the sham group, the expression levels of TJPs (ZO-1 and Occludin) were downregulated and that of MMP-9 was significantly upregulated after ICH injury; compared with the ICH + vehicle group, SPD significantly decreased the expression of MMP-9 after ICH injury and increased the expression levels of TJPs (Figure 5A–F) (Figure S4). Additionally, the immunofluorescence co-localization results of ZO-1 and CD31 (an endothelial cell marker) in the area surrounding the hematoma verified that ICH could lead to the degradation of ZO-1 and CD31, while the co-staining results after SPD treatment displayed a significantly higher immunofluorescence intensity (Figure 5G). This is in accordance with the results of Western blot. We discovered that SPD reduces the expression of MMP-9 and safeguards the integrity of the BBB after ICH.

SPD Reduces Brain Edema and BBB Permeability Following ICH

Brain edema is determined by the brain water content. Compared with the sham group, the brain water content in the ipsilateral and contralateral hemispheres of the ICH + vehicle group increased significantly, while no significant difference was observed in the cerebellum (as an internal control). Compared with the ICH + vehicle group, SPD significantly decreased the brain water content in both hemispheres (Figure 6A). Evans blue extravasation and the albumin level in brain tissue are used to evaluate the permeability of the BBB. Our results indicated that, SPD treatment significantly attenuated blood-brain barrier permeability after ICH, as evidenced by both reduced albumin levels (Figure 6B and C) (Figure S5) and diminished EB extravasation (Figure 6D and E), compared to the ICH + vehicle group.

SPD Treatment Ameliorates Cell Death and Neurological Deficits

To further investigate SPD's neuroprotective effects post-ICH, brain tissue sections collected at 72 hours were subjected to TUNEL staining. Dual labeling of TUNEL and NeuN was used to assess neuronal death and overall cell death in perihematomal regions. The results indicated that compared with the sham group, the number of dead cells in the area surrounding the hematoma increased in the ICH + vehicle group. However, at the effective therapeutic dose, SPD could reduce the loss of brain cells and neurons (Figure 7A–C). To evaluate SPD's therapeutic effects, neurological deficits were assessed using the mNSS and the Corner Turn Test. At 24 hours post-ICH, both the ICH + vehicle and ICH + SPD groups exhibited significantly higher mNSS scores and right-turn rates compared to the sham group, but no differences were observed between the two ICH groups (ICH + vehicle vs ICH + SPD). By 72 hours, however, three-day SPD treatment markedly reduced mNSS scores and right-turn rates in the ICH + SPD group compared to the ICH + vehicle group (Figure 7D and E), indicating delayed but robust neuroprotection. The lack of early improvement (24 hours) may reflect the time required for SPD to modulate neuroinflammatory response and BBB repair.

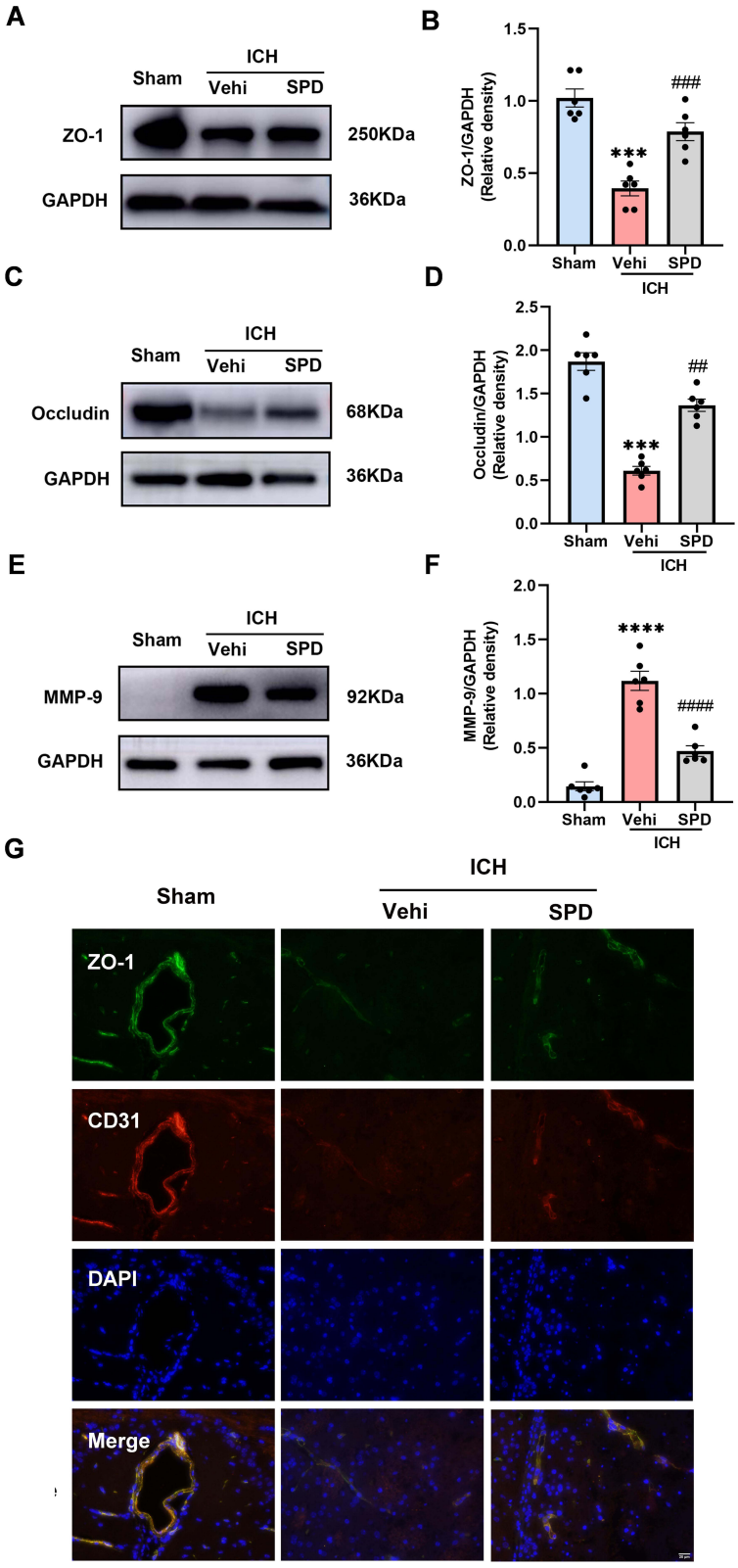

Figure 5 SPD protects the BBB integrity. (**A, C** and **E**) Representative Western blot bands of TJPs (Occludin and ZO-1) and MMP-9. (**B, D** and **F**) Quantitative analyses of relative protein expression level of Occludin, ZO-1 and MMP-9. n = 6 per group. (**G**) Representative microphotographs of immunofluorescence co-localization staining for ZO-1 (green) and CD31 (red) in the perihematomal area 72 hours after ICH. Scale bar = 20 μm. ***p < 0.001, ****p < 0.0001 vs sham. ##p < 0.01, ###p < 0.001, ####p < 0.0001 vs ICH + vehicle. Numerical data are shown as the mean ± SD. The difference between groups was analyzed using One-way ANOVA test.

https://doi.org/10.2147/JIR.S515256

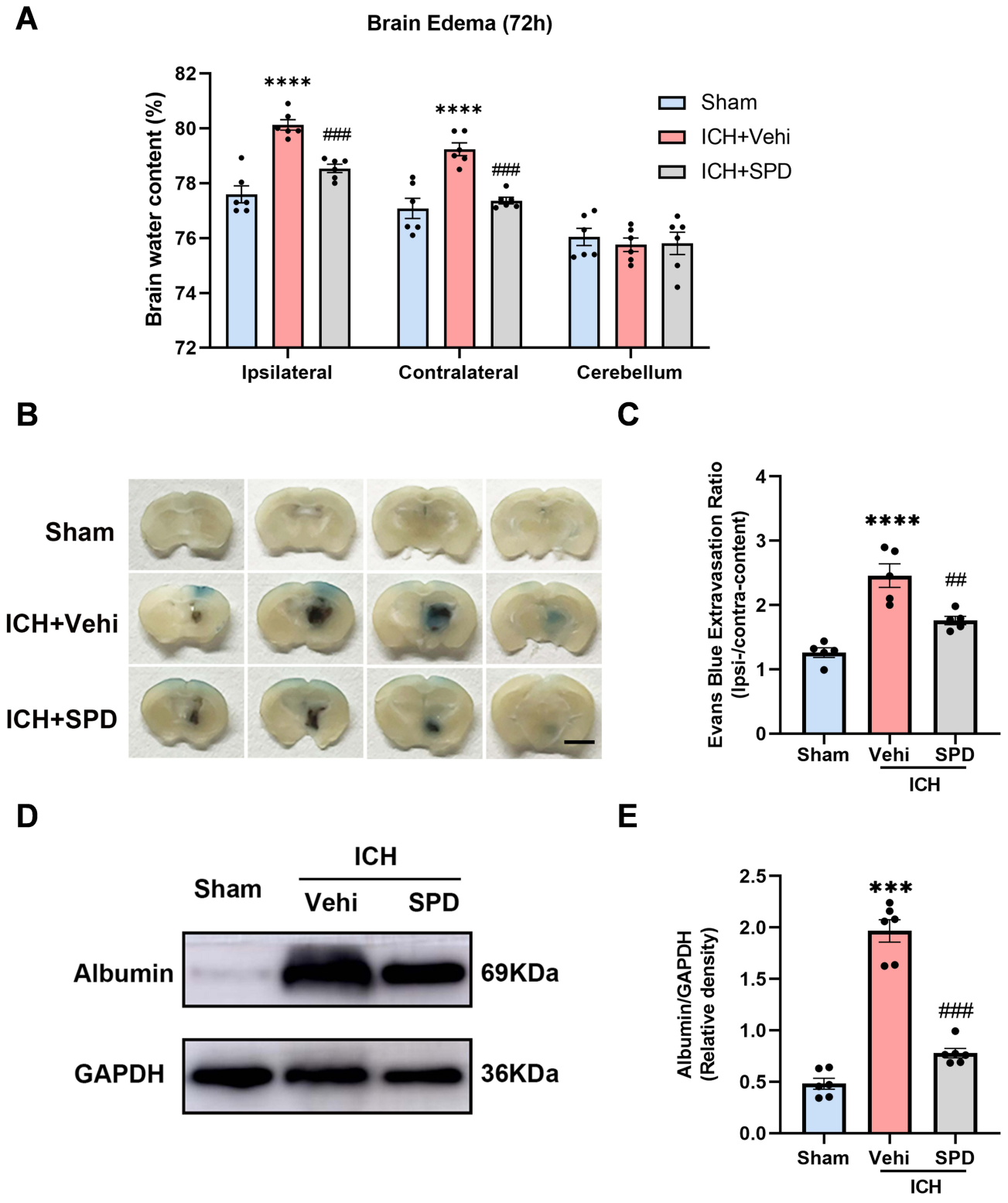

Figure 6 SPD alleviates the BBB leakage and brain edema. (**A**) Quantification of the brain water content. n = 6 per group. (**B**) Representative images of brain section after EB injection at 72 hours after ICH in mice. Scale bar =2.5 mm. (**C**) Quantification of EB leakage. n = 5 per group. (**D**) Representative Western blot results of Albumin in perihematomal region at 72 hours after ICH. (**E**) Quantitative analyses of relative protein expression level of Albumin. n = 6 per group. ***p < 0.001, ****p < 0.0001 vs sham. ##p < 0.01, ###p < 0.001 vs ICH + vehicle. Numerical data are shown as the mean ± SD. The difference between groups was analyzed using One-way ANOVA test.

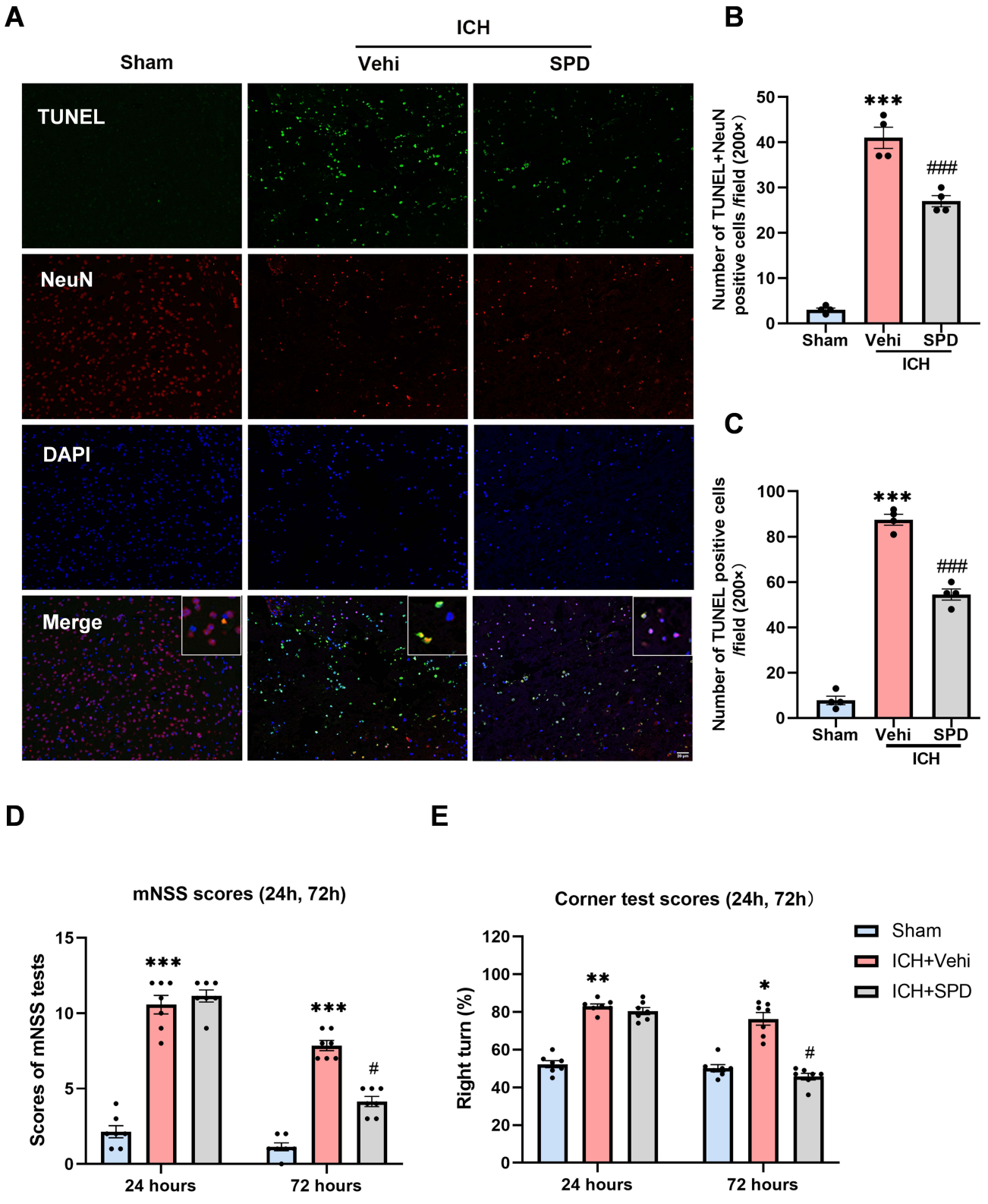

Figure 7 SPD treatment inhibits brain injury after ICH. (**A**) Representative microphotographs of TUNEL and NeuN positive cells in the peri-hematoma area 72 hours after ICH. Scale bar = 20 μm. (**B** and **C**) Quantification of the number of TUNEL$^+$ NeuN$^+$ and TUNEL$^+$ cells in perihematomal region, n = 4 per group. (**D**) Statistical analysis of mNSS scores at 24 hours and 72 hours after surgery in mice, n = 7 per group. (**E**) Statistical analysis of Corner Turning Test scores at 24 hours and 72 hours after surgery in mice, n = 7 per group. *p < 0.05, ** p < 0.01, ***p < 0.001 vs sham. #p < 0.05, ###p < 0.001 vs ICH + vehicle. Numerical data are shown as the mean ± SD. The difference between groups was analyzed using One-way ANOVA test.

https://doi.org/10.2147/JIR.S515256

Discussion

In the process of secondary brain injury following ICH, factors such as inflammation, oxidative stress, and BBB disruption interact, ultimately resulting in irreversible tissue damage and cell death.[41] In this study, we found that SPD treatment significantly reduced the hematoma volume, suppressed the death of brain cells, improved secondary brain injury, and ameliorated neurological deficits in the collagenase-induced ICH mouse model, and these beneficial effects might be associated with the inhibition of neuroinflammation and BBB damage.

The rapid and potent neuroinflammatory response after ICH is a crucial part in secondary brain injury.[42,43] Activated microglia/macrophages and infiltrated leukocytes release pro-inflammatory cytokines, including IL-1β, IL-6 and TNF-α, as well as chemokines and proteases such as MMP-9.[44,45] These inflammatory factors further activate the NF-κB signaling pathway in microglia, resulting in perforation of microglia and an accelerated release of intracellular inflammatory factors.[36] In summary, inflammatory cells and inflammatory molecules interact to mediate neuroinflammation-induced brain damage.

SPD is found highest in the human brain among the endogenous polyamines and involved in sustaining cellular and neuronal homeostasis.[46] An increasing number of experimental results have indicated the anti-inflammatory potential of SPD in the treatment of brain diseases. For example, in mouse models of Alzheimer's disease and experimental autoimmune encephalomyelitis, supplementation with SPD could combat neuroinflammation and exert neuroprotective functions.[17,47] Besides, in BV2 and macrophages, SPD regulates the NF-κB signaling pathway to inhibit inflammatory responses.[48–50]

Results from our animal experiments indicated that SPD suppressed the activation of microglia/macrophages, the infiltration of neutrophils, the phosphorylation of NF-κB and the release of pro-inflammatory cytokines (IL-1β, IL-6 and TNF-α), collectively demonstrating its anti-inflammatory effect. It is well-known that microglia/macrophages differentiate into two dynamically changing phenotypes after ICH: pro-inflammatory M1 phenotype and anti-inflammatory M2 phenotype.[51,52] To further explore the impact of SPD on the inflammatory response of microglia, we established an in vitro ICH model using BV2 cells. The results demonstrated that SPD inhibited the hemin-induced polarization of BV2 microglia toward M1 phenotype (iNOS, CD32) and reduced the release of pro-inflammatory cytokines (IL-1β, IL-6 and TNF-α). Together with in vivo data, these findings demonstrate SPD's anti-inflammatory efficacy in ICH.

In our animal experiments, SPD suppressed NF-κB phosphorylation, which aligns with its role in mitigating neuroinflammation. Mechanistically, SPD may reduce the tendency of the NF-κB complex to undergo nuclear translocation,[53] thereby reducing transcription of pro-inflammatory cytokines (IL-1β, IL-6, TNF-α) and MMP-9.[54,55] Furthermore, SPD shifts microglial polarization away from the pro-inflammatory M1 phenotype, which may be related to the inhibition of NF-κB and STAT1 signaling by SPD.[56] These multi-target actions further highlight SPD's potential as an anti-inflammatory agent for ICH.

The BBB is a barrier between the brain tissue and the blood vessels, composed of endothelial cells, TJPs, astrocytes, pericytes, and the basement membrane.[57,58] MMPs degrade the perivascular basement membrane, disrupt tight junction proteins, and degrade extracellular matrix and convert inflammatory mediators into their active forms after ICH, and the level of MMP-9 is confirmed to be associated with BBB damage in ICH patients.[59,60] In this experiment, SPD increased the expression of ZO-1, Occludin, and CD31 in the perihematomal area, decreased the expression of MMP-9, improved brain edema and reduced the exudation of EB dye and albumin. The positive impact of SPD on the integrity of the BBB can be explained by two mechanisms: 1. suppressing activated microglia/macrophages and infiltrated neutrophils, thereby inhibiting the attack of inflammatory factors on the components of the BBB;[61] 2. inhibiting the direct degradation of the basement membrane and tight junction proteins by MMP-9, thereby protecting the BBB itself.

While SPD has been studied in neurodegenerative diseases (eg, Alzheimer's and Parkinson's disease) for its anti-inflammatory and neuroprotective roles,[62,63] its therapeutic potential in ICH remains underexplored. Our study is the first to comprehensively assess SPD's effects on secondary brain injury post-ICH using both in vivo and in vitro models, filling a critical gap in this field. Moreover, beyond confirming SPD's anti-inflammatory effects (eg, reduced microglial activation, decreased IL-1β/IL-6/TNF-α levels), we uniquely demonstrate its ability to protect BBB integrity by upregulating tight junction proteins (ZO-1, Occludin) and suppressing MMP-9 expression. We revealed the dual protective mechanisms of SPD: anti-inflammation and BBB protection. Last but not least, as a naturally occurring polyamine with oral safety,[64] SPD offers a promising therapeutic avenue for ICH, particularly given the lack of effective treatments for secondary injury.

Our experiment still has several limitations. Firstly, we only observed the therapeutic efficacy of SPD in the 3-day ICH model. Additional studies are requisite to determine the long-term therapeutic effects of SPD. Secondly, we need to elucidate the molecular mechanisms underlying the anti-inflammatory effect of SPD in ICH. Thirdly, our study was limited to male and adult mice, and future research should explore the effects of SPD in female and aged mice to provide a more comprehensive understanding.

Conclusion

In conclusion, this study demonstrated that in ICH, continuous administration of SPD for three days significantly alleviated the secondary brain injury after ICH by suppressing neuroinflammation and protecting BBB integrity. Consequently, SPD holds significant potential as a treatment for ICH.

Data Sharing Statement

All original data generated in this study are presented in the article, any additional inquiries can be directed to the corresponding authors.

Ethics Statement

All experimental procedures were approved by the Ethics Committee of the Second Affiliated Hospital of Zhengzhou University (KY2024247). National Standards of the People's Republic of China (GB/T 35892–2018), Laboratory Animal —Guideline for Ethical Review of Animal Welfare, was the guidance for our animal care and protocols.

Acknowledgments

The authors acknowledge operating grant support from National Key Research and Development Program of China (grant no: 2018YFC1312200), the National Natural Science Foundation of China (grants no: 82071331 and 81870942), and from the Canadian Institutes of Health Research (VWY).

Author Contributions

All authors made a significant contribution to the work reported, whether that is in the conception, study design, execution, acquisition of data, analysis and interpretation, or in all these areas; took part in drafting, revising or critically reviewing the article; gave final approval of the version to be published; have agreed on the journal to which the article has been submitted; and agree to be accountable for all aspects of the work.

Disclosure

The authors declare no potential conflicts of interest with respect to the research, authorship and/or publication of this article.

References

1. Keep RF, Hua Y, Xi G. Intracerebral haemorrhage: mechanisms of injury and therapeutic targets. *Lancet Neurol*. 2012;11(8):720–731. doi:10.1016/S1474-4422(12)70104-7
2. Ji Y, Gao Q, Ma Y, et al. An MMP-9 exclusive neutralizing antibody attenuates blood-brain barrier breakdown in mice with stroke and reduces stroke patient-derived MMP-9 activity. *Pharmacol Res*. 2023;190:106720. doi:10.1016/j.phrs.2023.106720
3. Magid-Bernstein J, Girard R, Polster S, et al. Cerebral hemorrhage: pathophysiology, treatment, and future directions. *Circ Res*. 2022;130(8):1204–1229. doi:10.1161/CIRCRESAHA.121.319949
4. Qureshi AI, Mendelow AD, Hanley DF. Intracerebral haemorrhage. *Lancet*. 2009;373(9675):1632–1644. doi:10.1016/S0140-6736(09)60371-8
5. Bai Q, Sheng Z, Liu Y, Zhang R, Yong VW, Xue M. Intracerebral haemorrhage: from clinical settings to animal models. *Stroke Vasc Neurol*. 2020;5(4):388–395. doi:10.1136/svn-2020-000334
6. Zhang Y, Khan S, Liu Y, Wu G, Yong VW, Xue M. Oxidative stress following intracerebral hemorrhage: from molecular mechanisms to therapeutic targets. *Front Immunol*. 2022;13:847246. doi:10.3389/fimmu.2022.847246
7. Xue M, Yong VW. Neuroinflammation in intracerebral haemorrhage: immunotherapies with potential for translation. *Lancet Neurol*. 2020;19(12):1023–1032. doi:10.1016/S1474-4422(20)30364-1
8. Wang Y, Tian M, Tan J, et al. Irisin ameliorates neuroinflammation and neuronal apoptosis through integrin αVβ5/AMPK signaling pathway after intracerebral hemorrhage in mice. *J Neuroinflammation*. 2022;19(1). doi:10.1186/s12974-022-02438-6

9. Manaenko A, Yang P, Nowrangi D, et al. Inhibition of stress fiber formation preserves blood-brain barrier after intracerebral hemorrhage in mice. *J Cereb Blood Flow Metab*. 2018;38(1):87–102. doi:10.1177/0271678X16679169
10. Yenari MA, Xu L, Tang XN, Qiao Y, Giffard RG. Microglia potentiate damage to blood–brain barrier constituents. *Stroke*. 2006;37(4):1087–1093. doi:10.1161/01.STR.0000206281.77178.ac
11. Thiex R, Tsirka SE. Brain edema after intracerebral hemorrhage: mechanisms, treatment options, management strategies, and operative indications. *Neurosurg Focus*. 2007;22(5):E6. doi:10.3171/foc.2007.22.5.7
12. Li Z, Li M, Shi SX, et al. Brain transforms natural killer cells that exacerbate brain edema after intracerebral hemorrhage. *J Exp Med*. 2020;217 (12). doi:10.1084/jem.20200213
13. Li H, Wu J, Shen H, et al. Autophagy in hemorrhagic stroke: mechanisms and clinical implications. *Prog Neurobiol*. 2018;163-164:79–97. doi:10.1016/j.pneurobio.2017.04.002
14. Zhang Y, Xue M. Stereotaxic minimally invasive surgery for the successful treatment of intracerebral hemorrhage in children with brain herniation and case analysis. *J Neurorestoratol*. 2023;11(3):100072. doi:10.1016/j.jnrt.2023.100072
15. Madeo F, Bauer MA, Carmona-Gutierrez D, Kroemer G. Spermidine: a physiological autophagy inducer acting as an anti-aging vitamin in humans? *Autophagy*. 2019;15(1):165–168. doi:10.1080/15548627.2018.1530929
16. Hofer SJ, Simon AK, Bergmann M, Eisenberg T, Kroemer G, Madeo F. Mechanisms of spermidine-induced autophagy and geroprotection. *Nature Aging*. 2022;2(12):1112–1129. doi:10.1038/s43587-022-00322-9
17. Yang Q, Zheng C, Cao J, et al. Spermidine alleviates experimental autoimmune encephalomyelitis through inducing inhibitory macrophages. *Cell Death Differ*. 2016;23(11):1850–1861. doi:10.1038/cdd.2016.71
18. Zou D, Zhao Z, Li L, et al. A comprehensive review of spermidine: safety, health effects, absorption and metabolism, food materials evaluation, physical and chemical processing, and bioprocessing. *Compr Rev Food Sci Food Saf*. 2022;21(3):2820–2842. doi:10.1111/1541-4337.12963
19. Madeo F, Eisenberg T, Pietrocola F, Kroemer G. Spermidine in health and disease. *Science*. 2018;359(6374):eaan2788. doi:10.1126/science.aan2788
20. Guo X, Harada C, Namekata K, et al. Spermidine alleviates severity of murine experimental autoimmune encephalomyelitis. *Invest Ophthalmol Visual Sci*. 2011;52(5):2696–2703. doi:10.1167/iovs.10-6015
21. Noro T, Namekata K, Kimura A, et al. Spermidine promotes retinal ganglion cell survival and optic nerve regeneration in adult mice following optic nerve injury. *Cell Death Dis*. 2015;6(4):e1720. doi:10.1038/cddis.2015.93
22. Choi YH, Park HY. Anti-inflammatory effects of spermidine in lipopolysaccharide-stimulated BV2 microglial cells. *J Biomed Sci*. 2012;19(1):31. doi:10.1186/1423-0127-19-31
23. Wang J, Tsirka SE. Neuroprotection by inhibition of matrix metalloproteinases in a mouse model of intracerebral haemorrhage. *Brain*. 2005;128 (7):1622–1633. doi:10.1093/brain/awh489
24. Niu C, Jiang D, Guo Y, et al. Spermidine suppresses oxidative stress and ferroptosis by Nrf2/HO-1/GPX4 and Akt/FHC/ACSL4 pathway to alleviate ovarian damage. *Life Sci*. 2023;332:122109. doi:10.1016/j.lfs.2023.122109
25. Huang J, Zhang H, Zhang J, Yu H, Lin Z, Cai Y. Spermidine exhibits protective effects against traumatic brain injury. *Cell Mol Neurobiol*. 2020;40 (6):927–937. doi:10.1007/s10571-019-00783-4
26. Ziai WC. Hematology and inflammatory signaling of intracerebral hemorrhage. *Stroke*. 2013;44(6_suppl_1):S74–S78. doi:10.1161/STROKEAHA.111.000662
27. Liu Y, Li Z, Khan S, et al. Neuroprotection of minocycline by inhibition of extracellular matrix metalloproteinase inducer expression following intracerebral hemorrhage in mice. *Neurosci lett*. 2021;764:136297. doi:10.1016/j.neulet.2021.136297
28. Liu Y, Wang F, Li Z, Mu Y, Yong VW, Xue M. Neuroprotective effects of chlorogenic acid in a mouse model of intracerebral hemorrhage associated with reduced extracellular matrix metalloproteinase inducer. *Biomolecules*. 2022;12(8):1020. doi:10.3390/biom12081020
29. Deng S, Sherchan P, Jin P, et al. Recombinant CCL17 enhances hematoma resolution and activation of CCR4/ERK/Nrf2/CD163 signaling pathway after intracerebral hemorrhage in mice. *Neurotherapeutics*. 2020;17(4):1940–1953. doi:10.1007/s13311-020-00908-4
30. Feng D, Liu T, Zhang X, et al. Fingolimod improves diffuse brain injury by promoting AQP4 polarization and functional recovery of the glymphatic system. *CNS Neurosci Ther*. 2024;30(3):e14669. doi:10.1111/cns.14669
31. Liu H, Li C, Zhang X, et al. BMSC-Exosomes attenuate ALP dysfunction by restoring lysosomal function via the mTOR/TFEB Axis to reduce cerebral ischemia-reperfusion injury. *Exp Neurol*. 2024;376:114726. doi:10.1016/j.expneurol.2024.114726
32. Ou Q, Tang S, Zhu J, et al. Spermidine ameliorates osteoarthritis via altering macrophage polarization. *Biochimica et Biophysica Acta*. 2024;1870 (4):167083. doi:10.1016/j.bbadis.2024.167083
33. Zhang X, Zhang Y, Wang F, Liu Y, Yong VW, Xue M. Necrosulfonamide alleviates acute brain injury of intracerebral hemorrhage via inhibiting inflammation and necroptosis. *Front Mol Neurosci*. 2022;15.
34. Zhang Y, Liu Y, Zhang X, Yong VW, Xue M. Omarigliptin protects the integrity of the blood-brain barrier after intracerebral hemorrhage in mice. *J Inflamm Res*. 2023;16:2535–2548. doi:10.2147/JIR.S411017
35. Yu Y, Li X, Wu X, et al. Sodium hydrosulfide inhibits hemin-induced ferroptosis and lipid peroxidation in BV2 cells via the CBS/H2S system. *Cell Signalling*. 2023;104:110594. doi:10.1016/j.cellsig.2023.110594
36. Lei P, Li Z, Hua Q, et al. Ursolic acid alleviates neuroinflammation after intracerebral hemorrhage by mediating microglial pyroptosis via the NF-κB/NLRP3/GSDMD pathway. *Int J Mol Sci*. 2023;24(19):14771. doi:10.3390/ijms241914771
37. Jing Y-H, Yan J-L, Wang Q-J, et al. Spermidine ameliorates the neuronal aging by improving the mitochondrial function in vitro. *Exp Gerontology*. 2018;108:77–86. doi:10.1016/j.exger.2018.04.005
38. Guo Y, Dai W, Zheng Y, et al. Mechanism and regulation of microglia polarization in intracerebral hemorrhage. *Molecules*. 2022;27(20):7080. doi:10.3390/molecules27207080
39. Su Q, Su C, Zhang Y, et al. Adjudin protects blood–brain barrier integrity and attenuates neuroinflammation following intracerebral hemorrhage in mice. *Int immunopharmacol*. 2024;132:111962. doi:10.1016/j.intimp.2024.111962
40. Liu Y, Bai Q, Yong VW, Xue M. EMMPRIN promotes the expression of MMP-9 and exacerbates neurological dysfunction in a mouse model of intracerebral hemorrhage. *Neurochem Res*. 2022;47(8):2383–2395. doi:10.1007/s11064-022-03630-z
41. Li Z, Khan S, Liu Y, Wei R, Yong VW, Xue M. Therapeutic strategies for intracerebral hemorrhage. *Front Neurol*. 2022;13:1032343. doi:10.3389/fneur.2022.1032343

42. Zheng J, Lu J, Mei S, et al. Ceria nanoparticles ameliorate white matter injury after intracerebral hemorrhage: microglia-astrocyte involvement in remyelination. *J Neuroinflammation*. 2021;18(1):43. doi:10.1186/s12974-021-02101-6
43. Cao L, Zhang Y, Pi W, Yong VW, Xue M. Neuroinflammation and neurorestoration following stroke: molecular mechanisms and therapeutic approaches. *J Neurorestoratol*. 2025;13:100201. doi:10.1016/j.jnrt.2025.100201
44. Bai Q, Xue M, Yong VW. Microglia and macrophage phenotypes in intracerebral haemorrhage injury: therapeutic opportunities. *Brain*. 2020;143(5):1297–1314. doi:10.1093/brain/awz393
45. Xi G, Keep RF, Hoff JT. Mechanisms of brain injury after intracerebral haemorrhage. *Lancet Neurol*. 2006;5(1):53–63. doi:10.1016/S1474-4422(05)70283-0
46. Ghosh I, Sankhe R, Mudgal J, Arora D, Nampoothiri M. Spermidine, an autophagy inducer, as a therapeutic strategy in neurological disorders. *Neuropeptides*. 2020;83:102083. doi:10.1016/j.npep.2020.102083
47. Freitag K, Sterczyk N, Wendlinger S, et al. Spermidine reduces neuroinflammation and soluble amyloid beta in an Alzheimer's disease mouse model. *J Neuroinflammation*. 2022;19(1):172. doi:10.1186/s12974-022-02534-7
48. Luo J, Wang J, Zhang J, et al. Nrf2 deficiency exacerbated CLP-induced pulmonary injury and inflammation through autophagy- and NF-κB/PPARγ-mediated macrophage polarization. *Cells*. 2022;11(23):3927. doi:10.3390/cells11233927
49. Wang L, Cai J, Zhao X, et al. Palmitoylation prevents sustained inflammation by limiting NLRP3 inflammasome activation through chaperone-mediated autophagy. *Molecular Cell*. 2023;83(2):281–297.e210. doi:10.1016/j.molcel.2022.12.002
50. Wen Z, Fan L, Li Y, et al. Neutrophils counteract autophagy-mediated anti-inflammatory mechanisms in alveolar macrophage: role in posthemorrhagic shock acute lung inflammation. *J Immunol*. 2014;193(9):4623–4633. doi:10.4049/jimmunol.1400899
51. Yong HYF, Rawji KS, Ghorbani S, Xue M, Yong VW. The benefits of neuroinflammation for the repair of the injured central nervous system. *Cell Mol Immunol*. 2019;16(6):540–546. doi:10.1038/s41423-019-0223-3
52. Zhang R, Dong Y, Liu Y, et al. Enhanced liver X receptor signalling reduces brain injury and promotes tissue regeneration following experimental intracerebral haemorrhage: roles of microglia/macrophages. *Stroke Vasc Neurol*. 2023;8(6):486–502. doi:10.1136/svn-2023-002331
53. Guo X, Feng X, Yang Y, Zhang H, Bai L. Spermidine attenuates chondrocyte inflammation and cellular pyroptosis through the AhR/NF-κB axis and the NLRP3/caspase-1/GSDMD pathway. *Front Immunol*. 2024;15:1462777. doi:10.3389/fimmu.2024.1462777
54. Yu H, Lin L, Zhang Z, Zhang H, Hu H. Targeting NF-κB pathway for the therapy of diseases: mechanism and clinical study. *Signal Transduct Target Ther*. 2020;5(1):209. doi:10.1038/s41392-020-00312-6
55. Guo P, Liu L, Yang X, Li M, Zhao Q, Wu H. Irisin improves BBB dysfunction in SAP rats by inhibiting MMP-9 via the ERK/NF-κB signaling pathway. *Cell Signalling*. 2022;93:110300. doi:10.1016/j.cellsig.2022.110300
56. Shu J, Jiao Y, Wei W, Yan A. Spermidine inhibits M1 microglia polarization in a mouse model of parkinson's disease and BV2 cells via NF-κB/STAT-1 pathway. *Brain Behav*. 2025;15(3):e70410. doi:10.1002/brb3.70410
57. Daneman R. The blood-brain barrier in health and disease. *Ann Neurol*. 2012;72(5):648–672. doi:10.1002/ana.23648
58. Xu Y, Wang K, Dai Y, et al. Peripheral cytokine interleukin-10 alleviates perihematomal edema after intracerebral hemorrhage via interleukin-10 receptor/JAK1/STAT3 signaling. *CNS Neurosci Ther*. 2024;30(6). doi:10.1111/cns.14796
59. Shan Y, Tan S, Lin Y, et al. The glucagon-like peptide-1 receptor agonist reduces inflammation and blood-brain barrier breakdown in an astrocyte-dependent manner in experimental stroke. *J Neuroinflammation*. 2019;16(1):242. doi:10.1186/s12974-019-1638-6
60. Liu Y, Qi L, Li Z, Yong VW, Xue M. crosstalk between matrix metalloproteinases and their inducer EMMPRIN/CD147: a promising therapeutic target for intracerebral hemorrhage. *Transl Stroke Res*. 2023:1–11.
61. Kang L, Yu H, Yang X, et al. Neutrophil extracellular traps released by neutrophils impair revascularization and vascular remodeling after stroke. *Nat Commun*. 2020;11(1):2488. doi:10.1038/s41467-020-16191-y
62. Yang X, Zhang M, Dai Y, et al. Spermidine inhibits neurodegeneration and delays aging via the PINK1-PDR1-dependent mitophagy pathway in C. elegans. *Aging*. 2020;12(17):16852–16866. doi:10.18632/aging.103578
63. Sharma S, Kumar P, Deshmukh R. Neuroprotective potential of spermidine against rotenone induced Parkinson's disease in rats. *Neurochem Int* 2018;116:104–111. doi:10.1016/j.neuint.2018.02.010
64. Schwarz C, Stekovic S, Wirth M, et al. Safety and tolerability of spermidine supplementation in mice and older adults with subjective cognitive decline. *Aging*. 2018;10(1):19–33. doi:10.18632/aging.101354